Paper

External Dose to Recovery Teams Following a Wide-area Nuclear or Radiological Release Event

Michael D. Kaminski,[1] Keith Sanders,[2] Katherine Hepler,[1] Matthew Magnuson,[3] and Jeremy Slagley[2]

Abstract—**The common radionuclide ^{137}Cs is a gamma-ray source term for nuclear reactor accidents, nuclear detonations, and potential radionuclide dispersal devices. For wide-area contamination events, one remediation option integrates water washing activities with on-site treatment of water for its immediate reuse. This remediation option includes washing building and roadways via firehose, collecting the wash water, and passing the contaminated water through chemical filtration beds. The primary objective of this study was to quantify the dose incurred to workers performing a remediation recovery effort for roadways and buildings following a wide-area release event. MicroShield® was employed to calculate the dose to workers at the roadway level and to calculate total dose rates while performing washing activities. This study finds that for a realistic contamination scenario for a wide area of a large urban environment, decontamination crews would be subjected to <220 μSv per person, much less than the 50,000 μSv limit for occupational dose. By extrapolation, one decontamination team of 48 people could continue washing operations on a total of 2.8 km^2 before reaching their incurred annual dose limits. Though it is unrealistic to assign one team that entire area, we can conclude external dose will not limit worker deployment given the range of contamination levels adopted in this study.**
Health Phys. 120(6):591–599; 2021

Key words: ^{137}Cs; accidents, nuclear; dose, external; occupational safety

INTRODUCTION

In 1947, the first United Nations document defining weapons of mass destruction recognized the potential malicious use of radiological dispersal devices (Carus 2012). Today, the threat of attack using radiological dispersal devices (RDD) or improvised nuclear devices (IND) and risk presented by nuclear reactor accidents persists. A number of studies present dosimetry calculations for various contamination scenarios and remediation options (Kamboj et al. 2009; Thiessen et al. 2009b and c; Furuta and Takahashi 2015), including studies on populations near Fukushima Daiichi (Harada et al. 2014; Kinase et al. 2015; Naito et al. 2016). While these important investigations provide valuable information for stakeholders, studies to quantify the dose incurred by workers performing a remediation effort for roadways and buildings appear to be limited to workers in villages near Fukushima Daiichi (Suto et al. 2013; Tsubokura et al. 2013; Etherington et al. 2014; Sakumi et al. 2015). The present study focuses on the common radionuclide ^{137}Cs because this radionuclide is a dominating, long-term gamma-ray source term for nuclear detonations, some radionuclide dispersal devices, and nuclear reactor accidents (Leikin et al. 2003). Prior studies showed that water washing methods may remove between 20 and 80% of cesium contaminations depending on the physicochemical form of the contamination (Thiessen et al. 2009a; Kaminski et al. 2016). Recently, the US Environmental Protection Agency (EPA) has been evaluating decontamination methods (US EPA 2020a). One such method integrates water washing activities with on-site treatment of water for its immediate reuse (Kaminski et al. 2015). This process includes washing buildings and roadways via firehose, collecting the wash water, and passing the contaminated water through ad hoc chemical filtration beds, co-located with wash down operations, designed to quantitatively remove radioactive cesium ions. The purpose of this paper is to elucidate the viability of this approach by modeling external exposure to decontamination workers following a release event in an urban canyon. Assuming a uniform dispersion of material across all vertical (building facades) and horizontal (roadways) surfaces, MicroShield® was employed to calculate the dose

[1]Strategic Security Sciences Division, Argonne National Laboratory, 9700 S. Cass Avenue, Lemont, IL 60439; [2]Air Force Institute of Technology, Department of Systems Engineering and Management, 2950 Hobson Way, Wright-Patterson Air Force Base, OH 45433; [3]US Environmental Protection Agency, Office of Research and Development, Center for Environmental Solutions and Emergency Response, Homeland Security & Materials and Management Division, 26 W. Martin Luther King Drive, Cincinnati, OH 45268.

The authors declare no conflicts of interest.

For correspondence contact M. D. Kaminski, Strategic Security Sciences Division, Argonne National Laboratory, 9700 S. Cass Avenue, Lemont, IL 60439, or email at **kaminski@anl.gov**.

(*Manuscript accepted* 30 *September* 2020)

Supplemental digital content is available in the HTML and PDF versions of this article on the journal's website www.health-physics.com.

0017-9078/21/0

DOI: 10.1097/HP.0000000000001381

to workers at the roadway level and to calculate total absorbed rates while performing washing activities. Using various cases of decontamination efficacy and the location of contaminant filtration beds, the incurred dose was calculated.

METHODS

The scenario modeled a person standing on a roadway between two tall buildings (Fig. 1). A uniform distribution of radioactive ^{137}Cs covers the roadway (122 m long and 27.4 m wide) roughly the length of one standard US city block and two building facades (122 m long and 30.48 m tall) facing the roadway. The exposure rate was modeled incrementally before, during, and after a washing decontamination by hypothetical personnel. Cesium washed from the surface was quantitatively captured directly into filtration beds at the roadway level (described in detail in Kaminski et al. 2015), providing another source term. Then, the model could estimate the expected total absorbed dose to emergency crews performing the washing activities. Variables included the total residual radioactivity on surfaces over time due to the decontamination efficacy (percentage of contamination removed by wash methods), location of the workers, wash areal rates, different filter bed options and locations, and worker shift duration. Dose rates from resuspended material and rain-down aerosols generated from the impact of sprayed water on the surfaces, and then possibly depositing on the workers' personal protective equipment, are expected to be insignificant to the presented results. For example, this wash down technique was demonstrated by firefighter crews (US EPA 2016a), and the authors observed little to no rain-down aerosol to the crews operating the hoses.

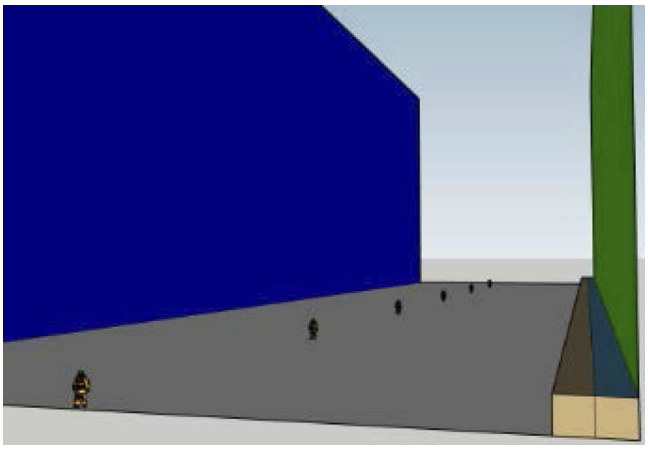

Fig. 1. Conceptual model of worker exposure points (to scale). The roadway (gray panel) separates Building 1 (green panel, right) and Building 2 (turquoise panel, left). A row of filter beds lines the base of Building 1 with a single row of sand-filled beds that serve as shielding to the workers. Workers are shown in the drawing at dose point 1 (back of image) through dose point 6 (forefront of image) (images of firefighters courtesy of 3D Firemen/Firefighter open source art and 3D sculpture project).

Modeling inputs

Source geometry and radiation exposure were modeled in MicroShield® (v10.04, Grove Software, Lynchburg, VA). Even though ^{137}Cs presents an internal dose health risk via ingestion or inhalation, those routes of exposure were not considered during this study since it is assumed that wash crews would be wearing appropriate personal protective equipment. Moreover, studies on Fukushima decontamination workers suggest that internal contamination from inhaled dust poses minimal additional risk (Tsubokura et al. 2013; Yasui 2013) with half-masks providing the necessary protection in areas of high surface contamination. The absorbed dose in air was obtained from the exposure rate in air [in roentgen (R) per hour] using the factor of 0.876 rad/R and then converted to SI units. The quality factor of ^{137}Cs gamma radiation is 1, and the "f-factor" for tissue was assumed unity. MicroShield reported the exposure and absorbed dose rates accounting for buildup.

Exposure source

The 2006 National Planning Scenario 11 (US DHS 2006) provided the basis for the total ^{137}Cs released in a potential dirty bomb incident. The planning scenario predicts that radioactivity concentrations could be 185–1,850 kBq m^{-2}, with hot spots 3,700-18,500 kBq m^{-2}. For all calculations herein, the model assumed an initial contamination concentration of all exterior surfaces of 1,850 kBq m^{-2}. To span a range of wash efficiencies, the model assumed activity concentrations of 30%, 50%, and 80% of the original for the decontamination efficiency applied to all surfaces.

Source geometry

The contaminated roadway and exterior contaminated facades of the buildings were represented as horizontal and vertical rectangular area sources (Fig. 1) in relation to a person standing on the roadway between Building 1 and Building 2. We used sensitivity analysis in MicroShield to provide exposure rates derived from the building facade in increments of roughly one story (3.05 m). A limitation of MicroShield® is that the dose point must be outside the source. Thus, to account for the exposure from the roadway, the horizontal source was broken into two 13.4-m by 122-m sources and then added together (Fig. 2).

A variable fraction of contamination will be transferred to the wash waters during washing operations that will pass through a series of filtration beds containing reactive fill material to sorb the radioactive cesium (Jolin and Kaminski 2016). Two geometries were compared for the filtration beds. The first was a row of cells (0.91 m × 122 m × 0.64 m) along Building 1 to catch the wash water as it collects at the base (Fig. 3). The second was a rectangular cuboid 0.91 m wide × 0.91 m long × 0.64 m tall with its corner vertex located at x = 1.86 m, z = 61 m, which would require all water to be collected and pumped through this single unit.

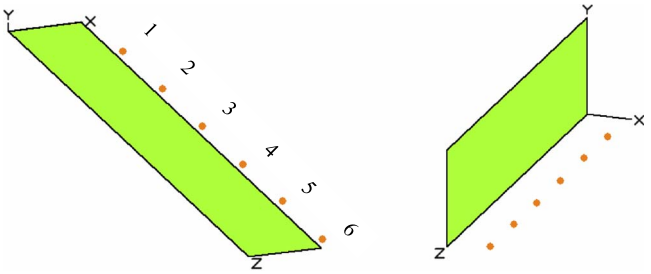

Fig. 2. (left) One-half the roadway modeled as a horizontal rectangular plane and (right) the building facade modeled as a vertical plane. The orange dots denote the position of the calculated exposure and dose points 1–6.

One cuboid cell or rows of cells (Figs. 1 and 3) containing sand is modeled between the filter bed(s) and the dose point to serve as shielding material.

Source composition

Using 1,850 kBq m^{-2}, the workers received exposure from 1.376×10^7 kBq total found on the two building facades (3,716 m^2 per building facade) and 6.179×10^6 kBq on the roadway (3,345 m^2). During and after wash down operations, the activity removed from the surfaces is transferred to the filter bed to compute the source term associated with the filter bed. If one assumes quantitative transfer of the ^{137}Cs from the surfaces to the wash water, the resulting concentration and volume can be captured successfully in a single cuboid filter bed 0.54 m^3 in volume.[4] For modeling purposes, MicroShield® assumed a homogeneous distribution of the activity within the volumetric source term of the filtration beds, which are filled with a mixture of sand and clay (sand density $\rho = 2.0$ and for clay $\rho = 0.67$ g cm^{-3}). The filtration bed material was a 70:30 sand-to-clay ratio ($\rho = 1.6$ g cm^{-3}).

Exposure locations

The MicroShield® software allows for the simultaneous calculation of six dose points on each run. For the pre-decontamination and post-decontamination comparison, the dose points are six evenly spaced locations down the centerline of the roadway (Fig. 1) with fixed x = 1,400 cm away from the facade at a height y = 152 cm above the roadway, and varying distance down the roadway at z = 20.0 m, 41.0 m, 61.0 m, 81.0 m, 100 m, and 122 m defining dose points 1–6, respectively. Note that dose point 1 is located 20 m from the beginning of the road, and dose point 6 is located at the end of the road (Fig. 2). Prior to decontamination, there are three modeled sources: the roadway and the facades of Building 1 and 2, all uniformly distributed with 1,850 kBq m^{-2}. During and after decontamination, the modeled sources are initial and residual contamination on the roadway and facades of Building 1 and 2 and the filtration beds containing the ^{137}Cs removed from the roadway and building facades.

[4]US Environmental Protection Agency. Simple scenario planning program for water recycling in nuclear release scenarios. Washington, DC: US Environmental Protection Agency; 2020b (in press).

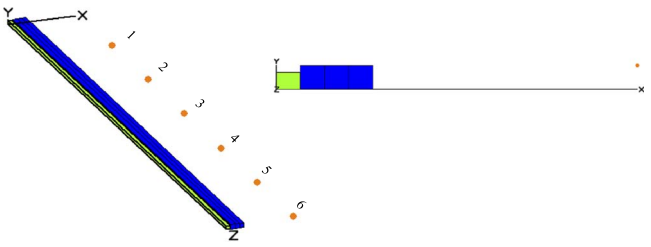

Fig. 3. Perspective (left) and side view (right) of line source of filtration cells along the facade of Building 1. In this example, three rows of sand-filled cells provided shielding (blue). The orange dots are the exposure points (1–6) along the centerline of the roadway.

Worker exposure time

The external dose to the workers is a function of exposure rate and the time (Table 1) needed to perform the decontamination wash of the roadway (Δt_{Rd}), Building 1 (Δt_{Blg1}), and Building 2 (Δt_{Blg2}). Using anticipated wash rates ($\dot{W}$) of 40, 60, or 80 m^2 h^{-1} (US EPA 2016b), the total time was calculated from the total area (A) of decontamination (3,345 m^2 for the roadway and 3,716 m^2 per building facade) as:

$$\Delta t_{Rd} = \frac{A_{Rd}}{\dot{W}_{40,60,80}}, \quad \Delta t_{Blg1} = \frac{A_{Blg1}}{\dot{W}_{40,60,80}}, \quad \Delta t_{Blg2} = \frac{A_{Blg2}}{\dot{W}_{40,60,80}}. \quad (1)$$

Worker dose rates

The total absorbed dose was calculated from the average pre- and post-decontamination absorbed dose rates from each of the sources. Rather than workers standing in the middle of the roadway, the model calculated the dose to workers standing at 1.86 m, 7.6 m, and 13.7 m from Building 1 at dose point 3 (3a, 3b, and 3c, respectively, Fig. 4).

Decontamination was performed first for the roadway (*Rd*) and then for each building facade in turn (*Blg1*, *Blg2*) with radioactivity filling the filtration bed (*Bed*). The resultant total absorbed dose D_{Tot} (in μGy) was the sum of the average dose $\overline{D}$ resulting from washing the roadway, Building 1, and Building 2 or,

$$D_{Tot}[\mu Sv] = \overline{D}_{Rd} + \overline{D}_{Blg1} + \overline{D}_{Blg2} = \overline{\dot{E}}_{\Delta Rd}\Delta t_{Rd} + \overline{\dot{E}}_{\Delta Blg1}\Delta t_{Blg1} + \overline{\dot{E}}_{\Delta Blg2}\Delta t_{Blg2}, \quad (2)$$

where $\overline{\dot{E}}_{\Delta}$ is the average absorbed dose rate experienced for the duration of washing of the roadway, Building 1, and

Table 1. Time (Δt) required to perform decontamination of the roadway surface (*Rd*) and a building facade (*Blg1*, *Blg 2*) based on wash rates.

	A_{Rd} = 3,345 m^2		$A_{Blg1} = A_{Blg2}$ = 3,716 m^2	
Wash rate m^2 h^{-1}	Δt_{Rd} (h)	Number 8-h shifts	$\Delta t_{Blg1} = \Delta t_{Blg2}$ (h)	Number 8-h shifts
40	83.6	11	92.9	12
60	55.7	7	61.9	8
80	41.8	6	46.5	6

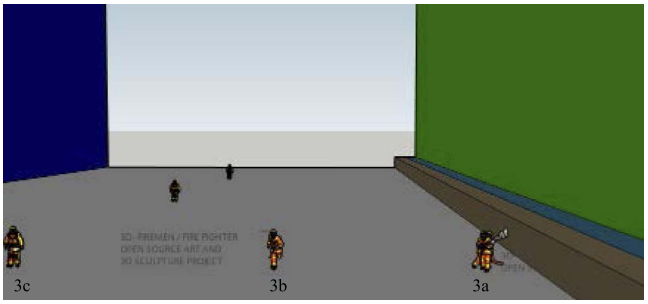

Fig. 4. Drawing showing workers standing at dose point 3 progressively closer to Building 1 facade (worker standing at dose points 1 and 2 shown also) (images of firefighters courtesy of 3D Firemen/ Firefighter open source art and 3D sculpture project).

Building 2. The value of $\overline{\dot{E}}_{\Delta}$ was estimated by taking the average absorbed dose rate to workers before and after completing each step in the decontamination wash. The average absorbed dose rate during, for instance, roadway washing $\overline{\dot{E}}_{\Delta Rd}$ was the average of the absorbed dose rate calculated before roadway operations were initiated ($\overline{\dot{E}}_{Pre}$) and after the roadway ($\overline{\dot{E}}_{Rd}$) was completed. The logic follows for $\overline{\dot{E}}_{\Delta Blg1}$, calculated from the average absorbed dose rate before beginning washing of Building 1 ($\overline{\dot{E}}_{Rd}$) and after completing Building 1 ($\overline{\dot{E}}_{Blg1}$), and $\overline{\dot{E}}_{\Delta Blg2}$, calculated from the average absorbed dose rate before beginning washing of Building 2 ($\overline{\dot{E}}_{Blg1}$) and after completing Building 2 ($\overline{\dot{E}}_{Blg2}$), or

$$\overline{\dot{E}}_{\Delta Rd}=\frac{\overline{\dot{E}}_{Pre}+\overline{\dot{E}}_{Rd}}{2},\quad \overline{\dot{E}}_{\Delta Blg1}=\frac{\overline{\dot{E}}_{Rd}+\overline{\dot{E}}_{Blg1}}{2},\quad \overline{\dot{E}}_{\Delta Blg2}=\frac{\overline{\dot{E}}_{Blg1}+\overline{\dot{E}}_{Blg2}}{2}. \quad (3)$$

The average absorbed dose rates before starting operations and after completing washing of each surface is calculated as the average absorbed dose rates $\dot{E}$ at each of the three dose points (3a, 3b, 3c) resulting from radioactivity emanating from the three surfaces and any coming from the filter bed as:

$$\overline{\dot{E}}_{Pre}=\sum_{j=3a}^{3c}\left(\frac{\dot{E}_{Rd,}i,j+\dot{E}_{Blg1,}i,j+\dot{E}_{Blg2,}i,j}{3}\right) \quad (4)$$

$$\overline{\dot{E}}_{Rd}=\sum_{j=3a}^{3c}\left(\frac{\dot{E}_{Rd,}f,j+\dot{E}_{Blg1,}i,j+\dot{E}_{Blg2,}i,j+\dot{E}_{Bed,}Rd,j}{3}\right) \quad (5)$$

$$\overline{\dot{E}}_{Blg1}=\sum_{j=3a}^{3c}\left(\frac{\dot{E}_{Rd,}f,j+\dot{E}_{Blg1,}f,j+\dot{E}_{Blg2,}i,j+\dot{E}_{Bed,}Blg1,j}{3}\right) \quad (6)$$

$$\overline{\dot{E}}_{Blg2}=\sum_{j=3a}^{3c}\left(\frac{\dot{E}_{Rd,}f,j+\dot{E}_{Blg1,}f,j+\dot{E}_{Blg2,}f,j+\dot{E}_{Bed,}Blg2,j}{3}\right), \quad (7)$$

where the subscript i refers to the absorbed dose rate from that surface before decontamination and f refers to the absorbed dose rate from that surface after decontamination.

RESULTS

The results reflect differing exposure rates as the decontamination progresses and workers wash the radioactivity from the sides of the building and collect it in the filtration beds. At the beginning of the decontamination process, there are three large unshielded sources of exposure with planar geometry: the roadway and each of the two building facades. During the decontamination process, additional source terms are created with the ^{137}Cs that is collected in either the single filter bed unit or a row of beds running along the length of the facade.

Exposure rates as a function of contamination height

Sensitivity analysis of the facades found that for a 20-story building facade with a uniform surface concentration, 75% of the exposure rate at ground level comes from the activity in the first 10 stories of the building. For a 12-story building, 90% of the exposure rate at ground level emanates from the first nine stories. For this study, the effective vertical height of the source was set at 30.48 m or 10 stories for subsequent calculations, which is near the limit of reach for ladder truck firehose equipment.

Dose from filter bed units

The model calculated a dose rate from a single filter bed (0.54 m^3) of 60 μGy h^{-1} at 1 m with a content of 6.88×10^6 kBq from one building facade. Adding a 0.91-m-deep cuboid unit containing sand as shielding material between the filter bed and the dose point reduced the dose to 1.9×10^{-4} μGy h^{-1} at 1 m from the source. The dose rate for a filter bed unit containing the total 1.99×10^7 kBq found on the roadway and both building facades was 213 μGy h^{-1} at 1 m, but it was only 3.5 μGy h^{-1} at 1 m with a sandbag shield wall (0.36 m deep) and 8.8×10^{-4} μGy h^{-1} at 1 m with the sand-filled cuboid (0.91-m-thick) shielding. Similarly, a single row of cuboid bed filters (Fig. 1) containing 6.88×10^6 kBq uniformly distributed within its volume produced a dose of 0.14 μGy h^{-1} at the centerline of the roadway. This dose was reduced to 0.93×10^{-6} μGy h^{-1} when a single row of sand-filled cuboid filters was placed as shielding. Therefore, by providing simple shielding options for the filter beds, one can eliminate these source terms.

Dose rates from contaminated roadway and facades

To start, the dose rates to someone standing in the middle of the roadway at the centerline between the buildings (dose point 3) is 2.4 μGy h^{-1} (69% of total) from the roadway and 0.56 μGy h^{-1} (15% of total) from each building facade (Table 2). The lower dose rate reported for point 6 is due to its location at the end of the roadway (z = 122 m).

Dose rates from a wide area contamination and elevated background

To see the effect of much larger contaminated areas on the dose rates, the building length was extended by a factor

Table 2. Pre-decontamination dose rates resulting from the contaminated roadway and buildings to someone standing at roadway centerline.

	μGy h^{-1}			
Point	Roadway	Building 1	Building 2	Total
1	2.2	0.49	0.49	3.2
2	2.3	0.55	0.55	3.3
3	2.4	0.56	0.56	3.4
4	2.3	0.55	0.55	3.3
5	2.2	0.49	0.49	3.2
6	1.2	0.31	0.31	1.9

of 4 (488 m long) at the same contamination concentration, producing a highest dose rate of 0.56 μGy h^{-1} to someone standing in the middle of the roadway. If the contaminated facade of the building was extended in length by a factor of 10, the calculated dose from it would be 0.67 μGy h^{-1} to someone standing 13.7 m away midline down that stretch of buildings. Continuing in scale, if the roadway extends 10 times longer (1,220 m) and 10 times wider (274 m) to predict the unshielded dose coming from a larger swath of the city roadways, then the dose to that same person is 3.6 μGy h^{-1} (from 2.4 μGy h^{-1} in the initial model assumptions). Putting this information together to understand the dose rates from a network of roads, thereby estimating the elevated background in the work zone, the previous case was rerun with a brick wall placed 13.7 m from the worker to mimic a building facade to block the radiation emanating from adjacent roadways. The resultant dose rate from those shielded roadways increased by only 0.62 μGy h^{-1} from the base case of 2.4 μGy h^{-1} reported in Table 2. Thus, one may consider 0.62 μGy h^{-1} to be the background dose if the surfaces within the work zone had been quantitatively decontaminated.

Estimated total dose rates to emergency responders

To compute the dose to workers, the model assumes the worker will spend on average equal time spatially between the building facade and the middle of the street to perform washing and filtration activities. To do this, the model computed (Table 3) the dose rates at 0.91 m, 7.6 m, and at 13.7 m from Building 1 at the center point along the two building facades (dose point 3 in Fig. 1). Then, the average dose rate for someone working in the area, pre-decontamination, is estimated from the average total of the three chosen dose points or $\overline{\dot{E}}_{Pre}$ =4.0 μGy h^{-1}.

The resulting exposure rates varied only slightly with decontamination efficiency, so only the 80% case is reported for clarity (Table 4). In this exercise, the model assumed the street was washed first, then the facade of Building 1, and finally the facade of Building 2. All radioactivity was assumed to be instantaneously transferred into a row of filter beds placed along the base of Building 1 with and without shielding. As such, after decontamination of the roadway, the dose rate to the worker at point 3a closest to Building 1 is reduced from a pre-decontamination rate of 5.0 μGy h^{-1} to 3.2 μGy h^{-1}. After completing Building 2, the rate at 3a increases to 5.2 μGy h^{-1}, greater than the initial dose, if the filter bed were left unshielded. Shielded, the dose rate dropped to 3.2 μGy h^{-1} after roadway decontamination, 1.2 μGy h^{-1} after Building 1, and 0.96 μGy h^{-1} after Building 2 decontamination. The dose at the centerline of the street is much less in both the unshielded and shielded cases at no greater than 0.96 μGy h^{-1} after decontamination of Building 2.

On average, with shielding in front of the row of filter beds at the base of the building, the worker experiences a 47% reduction in dose rate following decontamination of the roadway (4.0 to 2.2 μGy h^{-}). After decontamination of Building 1, the average dose is reduced by 72% (4.0 to 1.1 μGy h^{-1}) and 80% after completing decontamination of Building 2 (4.0 to 0.79 μGy h^{-1}). The benefit of shielding is also evident as the average dose rate is reduced by only 38% after completing operations (4.0 to 2.5 μGy h^{-1}) if no shielding is available.

When we consider the single cuboid clay-sand filter bed placed against the building facade instead of a row of filter beds, the results show the effect of concentrating the source material (see Supplemental Tables S1–S2, http://links.lww.com/HP/A199). The dose rates from the single cuboid bed following decontamination of all surfaces with and without shielding were 1.8×10^{-3} and 91 μGy h^{-1}, respectively. Compared to columns 5 and 6 in Table 4, using the single cuboid bed resulted in a 53-fold increase in the dose rate.

Total expected dose as a function of worker location and wash rate

To relate these values to practice, it is useful to consider the wash rates (Table 1) and the average dose rates before and after decontamination of each surface for dose points 3a–3c (Table 4) to arrive at a total dose rate for a worker performing each step in the decontamination operation (Table 5). With shielding in place, the total dose for the entire operation was 237–482 μGy, depending on the wash rate $\dot{W}$. These values have been corrected for the single cuboid filter bed

Table 3. Initial (pre-decontamination) dose rates $\overline{\dot{E}}_{Pre}$ for workers at three points along the building centerline standing at 0.91 m, 7.6 m, and 13.7 m from Building 1.

	$\overline{\dot{E}}_{Pre}$ (μGy h^{-1})				
Dose Point	Roadway	Building 1	Building 2	Total	Avg. rate
3a	2.4	2.4	0.26	5.0	
3b	2.4	0.88	0.44	3.6	4.0
3c	2.4	0.53	0.53	3.5	

Table 4. Dose rates from sources following incremental decontamination of the roadway, Building 1, and Building 2. The row of sand-clay filters is assumed to run along the base of Building 1.

	Post decontamination of street (μGy h^{-1})							
Dose point	Roadway	Building 1	Building 2	Filter bed, no shield	Filter bed, with shield	Total, no shield	Total, with shield	Average, with shield
3a	0.47	2.36	0.30	0.13	8.2×10^{-6}	3.2	3.2	$\overline{\dot{E}}_{Rd}$
3b	0.47	0.85	0.41	0.19	1.6×10^{-5}	1.9	1.8	2.2
3c	0.47	0.56	0.56	0.10	8.5×10^{-6}	1.7	1.6	
	Post decontamination street and Building 1 (μGy h^{-1})							
3a	0.47	0.47	0.30	2.7	1.75×10^{-5}	4.0	1.2	$\overline{\dot{E}}_{Blg1}$
3b	0.47	0.17	0.41	0.40	3.2×10^{-5}	1.5	1.1	1.1
3c	0.47	0.11	0.56	0.20	1.8×10^{-5}	1.3	1.1	
	Post decontamination all surfaces (μGy h^{1})							
3a	0.47	0.47	0.06	4.2	2.6×10^{-5}	5.2	0.96	$\overline{\dot{E}}_{Blg2}$
3b	0.47	0.17	0.08	0.61	5.0×10^{-5}	1.3	0.70	0.79
3c	0.47	0.11	0.11	0.31	2.7×10^{-5}	0.96	0.70	

case and the increased dose concern for the unshielded bed (see Supplemental Table S3, http://links.lww.com/HP/A199).

DISCUSSION

The model assumption of 1,850 kBq m^{-2} and starting dose rate of 1.9–5.0 μGy h^{-1} (from an exposure rate of 0.22–0.57 mR h^{-1}) compares well with previous contamination events and studies. For example, Thiessen et al. modeled the contamination across Pripyat, near the Chernobyl reactor site, with measured contamination of 80–24,000 kBq m^{-2} of ^{137}Cs (Thiessen et al. 2009c). The predicted dose rate was 8–66 μGy h^{-1} outdoors. In another study, the authors simulated an RDD event where powdered ^{137}Cs was hypothetically dispersed, producing a surface contamination of 490-9,100 kBq m^{-2} downwind (Thiessen et al. 2009a) and dose rates up to 10 μGy h^{-1}. A separate hypothetical RDD event in an urban environment produced a calculated contamination of ~800–4,000 kBq m^{-2} (Kamboj et al. 2009), resulting in 8 μGy h^{-1} fields. Depositions due to the Fukushima reactor accident range to > 3,000 kBq m^{-2} and extending >20 km from the reactor site (Malins et al. 2016). Thus, the assumptions of this study and its results can be confidently extrapolated to a variety of release events with corrections of less than an order of magnitude.

The scenario depicted in this study assumed uniform contamination concentration across both horizontal and vertical surfaces. The appropriateness of this assumption can be debated as the details of a release event might be peculiar to that particular event and the actual deposition pattern difficult to predict. Avoiding details, one can imagine a scenario where radioactivity is carried high in the air and makes the tortuous path between buildings, suggesting that vertical facades might be impacted to a greater degree than the horizontal surfaces. On the other hand, fallout particles are well known to concentrate on horizontal surfaces over building walls (Roed 1990; see Table 2.2). Therefore, assuming a constant deposition concentration, as we have, may represent a conservative approach for the purpose of modeling dose. An important practical implication from this study is that exposure rates at the centerline of the roadway from activity on the building facades above 30 m are small (90% from up to the 9th floor in a 12-story building and 75% up to the 10th floor in a 20-story building) and, therefore, simplified calculations by considering only the activity up to the 10th floor where ladder trucks can reach.

Table 5. Total dose D_{Tot} during decontamination of roadway (*Rd*), Building 1 (*Blg1*), and Building 2 (*Blg2*) at $\dot{W}$ =40–80 m^2 h^{-1} wash rates with a row of filtration beds placed against the building facade.

Average dose rate (μGy/h) during decontamination				40 m^2 h^{-1} (μGy)			60 m^2 h^{-1} (μGy)			80 m^2 h^{-1} (μGy)			D_{Tot} (μGy) at $\dot{W}$		
	$\overline{\dot{E}}_{\Delta Rd}$	$\overline{\dot{E}}_{\Delta Blg1}$	$\overline{\dot{E}}_{\Delta Blg2}$	$\overline{D}_{Rd}$	$\overline{D}_{Blg1}$	$\overline{D}_{Blg2}$	$\overline{D}_{Rd}$	$\overline{D}_{Blg1}$	$\overline{D}_{Blg2}$	$\overline{D}_{Rd}$	$\overline{D}_{Blg1}$	$\overline{D}_{Blg2}$	40	60	80
No Shield	3.2	2.3	2.4	263	193	201	175	123	131	131	96	96	657	438	324
Shield	3.1	1.7	0.96	263	140	79	175	88	53	131	70	44	482	315	237

Even though the total surface area of the roadway sources made up less than a third of the total contaminated surface area, it was the single largest contributor to the overall dose rate (Table 2). Therefore, the effectiveness of the roadway decontamination strategy was the greatest influence on dose rates to workers, prompting us to simulate its decontamination first. This strategy is different than common site remediation practice where a top-down approach is used, because conventional wisdom would dictate that wash waters would flow down from the buildings and onto the horizontal surfaces. However, the wash concept described in Kaminski et al. (2015) uses flood control barriers to capture the water, limiting uncontrolled flow of contaminated water onto the roadway and, thus, supporting the practicality of initiating the roadway decontamination first without fear of re-contaminating it during building washing operations. Decontamination operations move the radioactivity to the filter beds, but dose rates show that filter bed design is not important to dose rates provided the filter bed is shielded properly. That makes the filter design a question of capacity and logistics. Certainly, waste management favors smaller volume. One sand-clay filter 0.54 m^3 in volume has the capacity needed to capture the incoming radioactivity in this scenario, a favorable configuration compared to a long row of diluted filter media. Also, a filter of this size can be handled very easily and transported with a dose of only 3.5 μGy h^{-1} at 1 m with sandbag shielding.

From Table 5, it is possible to estimate the total dose incurred by workers for various scenarios. To put this into practical perspective, Table 6 presents the dose for each areal wash rate $\dot{W}$ divided by the number of crews (3–8) working continuously for 18–35 shifts. For three crews, the shift is 8 h, while for nine crews, the shift is 3 h. The expected doses per crew member are 40–220 μGy without shielding and 30-160 μGy with shielding present. Including the elevated background would increase the reported dose values by approximately 50% on average. Supplemental Table S3, http://links.lww.com/HP/A199, reports a similar exercise for a single cuboid filtration bed, resulting in 730–3,880 μGy per crew member with no shielding and 30–160 μGy with shielding.

The model assumptions leading to these dose rates correspond to a realistic wide-area release scenario. Namely, calculations (see "Dose rates from a wide area contamination and elevated background") for a much larger roadway and building network had a minor effect on the dose (30% increase) resulting from the roadway and building facade sources. Thus, a more realistic wide area washing operation would be expected to have similar calculated doses.

Obviously, this is a highly idealized case since it does not account for any logistic considerations that would correct the constant areal wash rates assumed here to an actual average rate of progress during the washing of the roadways and buildings (such as delays and down times). To be protective of worker safety, we may multiply the above values by a factor of 3, resulting in a more conservative range of 90–480 μGy with shielding.

Table 6. Dose per crew member based on number of crews (3–8) with and without shielding for the line of cuboid filter beds placed against the building facade.

		Without shielding (μGy)						With shielding (μGy)					
		Number of crews						Number of crews					
Wash rate	Total shifts	3	4	5	6	7	8	3	4	5	6	7	8
40	35	220	160	130	110	90	80	160	120	100	80	70	60
60	23	150	110	90	70	60	50	110	90	80	60	50	50
80	18	110	80	70	50	50	40	80	60	50	40	30	30

In terms of practical applicability, the results in Tables 4 and 5 can be combined with a recent logistics study of washing operations (Hepler 2020) to obtain an enhanced understanding of doses workers may receive during a realistic decontamination activity. A primary goal of Hepler's study was to provide an order of magnitude estimate of the decontamination timeline and required resources to remediate an affected area, specifically a 0.0652 km^2 area of downtown Chicago, IL, contaminated with ^{137}Cs. Peak decontamination operations lasted 25 d and employed four decontamination teams. Decontamination operations were performed via fire hosing with an areal cleaning rate of 24 m^2 h^{-1} per 48-worker decontamination team. This size of team is required to meet requirements for logistics of crew rotations, equipment setup, and threshold working time (Hepler 2020) based on the physical demands of washing operations with personal protective equipment. Simulating the crew rotations with these logistical constraints predicted each worker would be in the contaminated area 4 h d^{-1}. The remaining time during a worker's shift was accounted for by rest periods in a contamination-free area; initial preparation before entering the contaminated area; and the transit time between a staging site, where preparatory actions occurred, and the contaminated site.

One decontamination team from Hepler's study would need to operate for 139 h to clean the street and 155 h to clean each building. Using the dose rates from Table 5 (see Supplemental Table S4, http://links.lww.com/HP/A199), this yields a total unshielded dose of 438 μGy cleaning the street, 350 μGy cleaning Building 1, and 368 μGy cleaning Building 2 (1,156 μGy total). For the shielded case, the total dose was 429 μGy cleaning the street, 254 μGy cleaning Building 1, and 149 μGy cleaning Building 2 (832 μGy total). To account for the fraction of time each worker was in the contaminated area during operations, the total dose can be divided by 6 (4 hours every 24-h period). Thus, the dose for each

of the 48 workers was 140 μGy for the shielded case and 193 μGy for the unshielded case. These results are comparable to those in Table 6.

Using the results in the previous paragraph, a practical estimate of the worker dose for Hepler's scenario can be made. The contaminated area in Hepler's study was 6.1 times the area of the street and buildings in this study, but four teams instead of one were deployed to clean the larger area. Therefore, the worker dose was only 1.5 times the results in the previous paragraph (210 μGy shielded or approximately 290 μGy unshielded). These accrued doses are small compared to the occupational dose limit of 50,000 μSv (US DHS 2008), or even a more conservative dose limit of 10,000 μSv. For the operating guidelines from Hepler (2020) applied to the contamination scenario in this study, one decontamination team could clean 43.8 km of street length shielded before workers received 50,000 μSv; 360 times the street length evaluated in this paper. If we assume typical street blocks are squares with 140-m side lengths, 43.8-km street length converts to a map area of about 2.8 km^2. Even if the contaminant levels increased 10-fold, each worker could be deployed for 1.8 y before reaching dose limits. This comparison shows that occupational dose equivalent limits will not be the limiting factor for decontamination worker deployment times for a range of potential contamination levels and the decontamination method used in this study.

CONCLUSION

This study provides important practical information on expected dose to workers remediating by using wash down operations after a wide area release event in an urban environment. A dose estimation model was developed for a wash system that relies on readily available supplies and captures activity from contaminated wash solution. This model was applied to a hypothetical, but realistic, scenario where a street length and two surrounding building facades were contaminated with ^{137}Cs. Sensitivity analysis of contaminated facades found the major contributor to worker dose is contamination deposited on the first 30.5 m of building height. Thus, this operation is possible with ladder trucks already available in fire departments that service such downtown areas. Evaluating radiation exposure from surrounding contaminated areas outside of the immediate area showed these areas contributed little to total pre-decontamination dose. The dose estimation model found that decontamination crews would be subjected to <220 μGy per person while cleaning the contaminated area, the equivalent of 120 m of an urban corridor, which is much less than the 50,000 μSv limit of occupational dose. Correlating these dose results with decontamination logistics information, theoretically one decontamination team of 48 people could continue operations for a total of 2.8 km^2 before reaching their dose limit, which is large percentage of many large cities around the world.

Acknowledgments—The research described in this article has been funded wholly or in part by the US Environmental Protection Agency interagency agreement DW-89-92439001 to Argonne National Laboratory. It has been subjected to review by the Office of Research and Development and approved for publication. Approval does not signify that the contents reflect the views of the Agency, nor does mention of trade names or commercial products constitute endorsement or recommendation for use. The submitted manuscript has been created by UChicago Argonne, LLC, Operator of Argonne National Laboratory ("Argonne"). Argonne, a US Department of Energy Office of Science laboratory, is operated under Contract No. DE-AC02-06CH11357. The US Government retains for itself, and others acting on its behalf, a paid-up nonexclusive, irrevocable worldwide license in said article to reproduce, prepare derivative works, distribute copies to the public, and perform publicly and display publicly, by or on behalf of the Government.

REFERENCES

Carus WS. Defining weapons of mass destruction. Washington, DC: National Defense University Center for the Study of Weapons of Mass Destruction; Occasional Paper No. 8; 2012.

Etherington G, Zhang W, Harrison J, Walsh L. Worker doses and potential health effects resulting from the accident at the Fukushima nuclear power plant in 2011. Internat J Radiat Biol 90:1088–1094; 2014.

Furuta T, Takahashi F. Study of radiation dose reduction of buildings of different sizes and materials. J Nucl Sci Technol 52: 897–904; 2015.

Harada KH, Niisoe T, Imanaka M, Takahashi T, Amako K, Fujii Y, Kanameishi M, Ohse K, Nakai Y, Nishikawa T, Saito Y, Sakamoto H, Ueyama K, Hisaki K, Ohara E, Inoue T, Yamamoto K, Matsuoka Y, Ohata H, Toshima K, Okada A, Sato H, Kuwamori T, Tani H, Suzuki R, Kashikura M, Nezu M, Miyachi Y, Arai F, Kuwamori M, Harada S, Ohmori A, Ishikawa H, Koizumi A. Radiation dose rates now and in the future for residents neighboring restricted areas of the Fukushima Daiichi nuclear power plant. Proc National Acad Sci 111:E914–E923; 2014.

Hepler KC. The effects of contaminant aging and decontamination logistics on remediation after a radiological dispersal event. Urbana, IL: University of Illinois; 2020. Dissertation.

Jolin WC, Kaminski M. Sorbent materials for rapid remediation of wash water during radiological event relief. Chemosphere 162:165–171; 2016.

Kamboj S, Cheng J-J, Yu C, Domotor S, Wallo A. Modeling of the emras urban working group hypothetical scenario using the RESRAD-RDD methodology. J Environ Radioact 100: 1012–1018; 2009.

Kaminski M, Mertz C, Kivenas N, Magnuson M. Irreversible wash aid additive for cesium mitigation: selection and/or modification of commercial off-the-shelf field portable waste water systems. Nuclear Engineering Division Report, Argonne National Laboratory. ANL/NE-15/13; 2015.

Kaminski M, Mertz C, Ortega L, Kivenas N. Sorption of radionuclides to building materials and its removal using simple wash solutions. J Environ Chem Eng 4:1514–1522; 2016.

Kinase S, Sato S, Sakamoto R, Yamamoto H, Saito K. Changes in ambient dose equivalent rates around roads at Kawamata town after the Fukushima accident. Radiat Protect Dosim 167: 340–343; 2015.

Leikin JB, McFee RB, Walter FG, Edsall K. A primer for nuclear terrorism. Disease-a-Month 49:485–516; 2003.

Malins A, Kurikami H, Kitamura A, Machida M. Effect of remediation parameters on in-air ambient dose equivalent rates when remediating open sites with radiocesium-contaminated soil. Health Phys 111:357–366; 2016.

Naito W, Uesaka M, Yamada C, Kurosawa T, Yasutaka T, Ishii H. Relationship between individual external doses, ambient dose rates and individuals' activity-patterns in affected areas in Fukushima following the Fukushima Daiichi nuclear power plant accident. PloS one 11:e0158879; 2016.

Roed J. Deposition and removal of radioactive substances in an urban area, NORD 1990:111. Riso National Laboratory, Denmark; 1990.

Sakumi A, Miyagawa R, Tamari Y, Nawa K, Sakura O, Nakagawa K. External effective radiation dose to workers in the restricted area of the Fukushima Daiichi nuclear power plant during the third year after the great east Japan earthquake. J Radiat Res 57:178–181; 2015.

Suto Y, Hirai M, Akiyama M, Kobashi G, Itokawa M, Akashi M, Sugiura N. Biodosimetry of restoration workers for the Tokyo Electric Power Company (TEPCO) Fukushima Daiichi nuclear power station accident. Health Phys 105:366–373; 2013.

Thiessen K, Andersson KG, Batandjieva B, Cheng J-J, Hwang W, Kaiser J, Kamboj S, Steiner M, Tomás J, Trifunovic D. Modelling the long-term consequences of a hypothetical dispersal of radioactivity in an urban area including remediation alternatives. J Environ Radioact 100:445–455; 2009.

Thiessen KM, Andersson KG, Charnock TW, Gallay F. Modelling remediation options for urban contamination situations. J Environ Radioact 100:564–573; 2009.

Thiessen KM, Arkhipov A, Batandjieva B, Charnock TW, Gaschak S, Golikov V, Hwang WT, Tomás J, Zlobenko B. Modelling of a large-scale urban contamination situation and remediation alternatives. J Environ Radioact 100:413–421; 2009.

Tsubokura M, Nihei M, Sato K, Masaki S, Sakuma Y, Kato S, Sugimoto A, Nomura S, Matsumura T, Miyazaki M, Hayano R, Shibuya K, Kami M, Sasaki T. Measurement of internal radiation exposure among decontamination workers in villages near the crippled Fukushima Daiichi nuclear power plant. Health Phys 105:379–381; 2013.

US Department of Homeland Security. National planning scenarios: created for use in national, federal, state, and local homeland security preparedness activities. Washington, DC: US Department of Homeland Security; Version 213; 2006.

US Department of Homeland Security. Planning guidance for protection and recovery following radiological dispersal device (RDD) and improvised nuclear device (IND) incidents. Fed Register 73:45029–45048; 2008.

US Environmental Protection Agency. Technical report for the demonstration of wide area radiological decontamination and mitigation technologies for building structures and vehicles. Washington, DC: US EPA; EPA/600/R-16/019; 2016a.

US Environmental Protection Agency. Integrated wash-aid, treatment, and emergency reuse system (IWATERS) for mitigation of soluble and particulate contaminants [online]. 2016b. Available at ***https://cfpub.epa.gov/si/si_public_record_report.cfm?dirEntryId=346170&Lab=NHSRC&searchAll=Homeland+Security&subject=Homeland+Security+Research&view=desc&sortBy=pubDateYear&count=25&showCriteria=1&searchall=radiological&submit=Search&startIndex=51&displayIt=Yes***. Accessed 25 May 2020.

US Environmental Protection Agency. Wide area remediation [online]. 2020a. Available at ***https://www.epa.gov/homeland-security-research/wide-area-remediation***. Accessed 7 December 2020.

Yasui S. Establishment of new regulations for radiological protection for decontamination work involving radioactive fallout emitted by the Fukushima Daiichi APP accident. J Occupat Environ Hygiene 10:D119–D124; 2013.

■■